Dalton Transactions

PAPER

View Article Online
View Journal | View Issue

Cite this: *Dalton Trans.*, 2018, **47**, 17357

New ferrocene-based 2-thio-imidazol-4-ones and their copper complexes. Synthesis and cytotoxicity†

D. A. Guk,[a] O. O. Krasnovskaya,[a] N. S. Dashkova,[a] D. A. Skvortsov,[a,b] M. P. Rubtsova,[a,b] V. P. Dyadchenko,[a] E. S. Yudina,[a] M. A. Kosarev,[a] A. V. Soldatov,[c] V. V. Shapovalov,[c] A. S. Semkina,[d] K. Y. Vlasova,[a] V. I. Pergushov,[a] R. R. Shafikov,[a] A. A. Andreeva,[f] M. Ya. Melnikov,[a] N. V. Zyk,[a] A. G. Majouga[a,e,f] and E. K. Beloglazkina *[a]

Received 3rd August 2018,
Accepted 13th November 2018

DOI: 10.1039/c8dt03164a

rsc.li/dalton

Synthesis, characterization (HRMS, NMR, EPR, XANES, UV-Vis spectroscopy, and electrochemistry), DNA and BSA binding and *in vitro* biological screening of two new ferrocene-incorporated thiohydantoin derivatives (**5** and **6**) and their copper coordination compounds are reported. The ferrocene-based thiohydantoin derivatives were prepared by copper-catalyzed azide alkyne cycloaddition reactions between alkynyl ferrocenes and 5-(*Z*)-3-(2-azidoethyl)-2-(methylthio)-5-(pyridin-2-ylmethylene)-1*H*-imidazol-4*H*-one. Alkynyl ferrocenes necessary for these syntheses were prepared by new procedures. Intermolecular redox reactions between the ferrocene fragment and copper(+2) coordinated ions were studied by different methods to determine the mechanism and kinetic constants of redox processes. Ferrocene-containing imidazolones (**5** and **6**) and their copper complexes were also tested for their *in vitro* cytotoxic activity against MCF-7 and A-549 carcinoma cells, and also against the noncancerous cell line Hek-293. The results showed modest cytotoxicity against the subjected cancer cell line compared with cisplatin. The ability of the obtained compounds to cause DNA degradation and cell apoptosis was investigated, and the distribution of cytosol/pellets was studied by AAS.

1. Introduction

Despite the fact that platinum-containing coordination compounds are successfully used in clinical practice, attempts to reduce their cytotoxic effect are often ineffective.[1,2] Therefore, it is important to search for new cytotoxic coordination compounds based on endogenous metals, which have lower general toxicity. The fact that transition metals such as iron, cobalt, zinc and copper are natural participants of intracellular metabolism makes the syntheses of metal complexes based on them and investigation of their biological activity expedient. At present, several coordination compounds of iron, cobalt[3] and copper[4] are at the first and second stages of preclinical trials as antitumor drugs.

According to the Web of Science, a number of publications devoted to the development of antineoplastic drugs based on copper continue to grow and exceed a number of similar publications devoted to other biogenic metals. Based on the early preclinical studies of copper(II) coordination compounds with *N*,*N*-bidentate heterocyclic ligands, such complexes are able to intercalate DNA with subsequent cleavage[5] and inhibit the growth of tumor cells.[6] Also, the concentration of copper ions in cancer cells is higher than in healthy cells, which is necess-

[a]*Chemistry Department, Lomonosov Moscow State University, Leninskie Gory 1/3, Moscow 119991, Russia*
[b]*Center of Life Sciences, Skolkovo Institute of Science and Technology, Skolkovo, Moscow, 143026, Russia*
[c]*Physics Department, Southern Federal University, Ulitsa Zorge, 5, Rostov 344000, Russia*
[d]*Pirogov Russian National Research Medical University (RNRMU) Ostrovitianov str. 1, Moscow, 117997, Russia*
[e]*National University of Science and Technology MISIS, Leninskiy prospect 4, Moscow 101000, Russia*
[f]*D. Mendeleev University of Chemical Technology of Russia, Miusskaya Ploshchad' 9, Moscow 125047, Russia*
†Electronic supplementary information (ESI) available. See DOI: 10.1039/c8dt03164a

ary for angiogenesis in malignant breast,[7,8] prostate,[9,10] large intestine,[10] and lung[11] tumors. Copper-containing complexes are inexpensive and have lower overall toxicity in comparison with platinum analogues.[12,13]

Most of the biologically active coordination compounds of copper described in the literature are Cu(II) complexes, due to the simplicity of the synthesis and the stability of such derivatives. At the same time, it is well known that the penetration of copper-containing therapeutic agents into a cell occurs when copper is in valence Cu(I), but not in the case of Cu(II),[14] which requires the presence of reducing agents. For example, ascorbic acid or glutathione (GSH) is able to reduce Cu(II) ions to Cu(I) before they penetrate into the cell.[15] Taking into account the fact that the effective penetration of the drug into the tumor cell leads to an increase in cytotoxicity and, as a result, the effectiveness of the drug, the principal task is the development of stable Cu(I)-containing cytotoxic compounds.

Previous studies of our research group were devoted to the derivatives of 2-thioimidazolones and 2-alkylthioimidazolin-4-ones, and coordination compounds of Cu(II,I) based on them, which showed an effective cytotoxic effect on tumor cells.[16–18] In this paper, we first propose a new approach for the stabilization of the +1 oxidation state of copper in such coordination compounds. In order to stabilize the copper ion in the monovalent state, we have proposed to introduce a redox-active fragment into the thiohydantoin ligand, which would make possible the intramolecular reduction of the copper ion from Cu(II) to Cu(I). Ferrocene was chosen as a redox-active fragment due to its biological activity and suitable electrochemical reduction potential ($E^0Cp_2Fe(II)/Cp_2Fe(III)$ = + 0.4 V), which is close to the reduction potential of copper(II) ions ($E^0Cu(II)\backslash Cu(I)$ = + 0.153 ± 0.39 V[19]). Thus, we have assumed the possibility of an intramolecular redox reaction $Fe^{2+} + Cu^{2+} \rightarrow Fe^{3+} + Cu^{1+}$. In addition, ferrocene itself is a pharmacophore fragment; ferrocene-containing compounds exhibit the antitumor activity against lymphocytic leukemia (P-388 cell line),[20] lung carcinoma (A549 cell line),[21] mammary adenocarcinoma (Ca-755[22] and the MCF-7[23] cell lines), and solid tumors.[24] Also, literature data suggest that the introduction of a ferrocene fragment into the antitumor drug structure can lead to an increase of the cytotoxic activity and, in some cases, the selectivity of the therapeutic agents.[25] So, one of the ferrocene-containing derivatives demonstrated the activity exceeding that of cisplatin.[26] In addition, ferrocene, due to its lipophilic nature, is able to facilitate further penetration of the coordination compound through the cell membrane. According to the data from ref. 27, the introduction of a redox-active ferrocene-containing derivative of natural amino acids into a structure of the curcumin complex with divalent copper leads not only to an increase of the cytotoxic activity of the conjugate compared to individual starting materials, but also to the accumulation of the ferrocene-containing conjugate in the cytosol.

We have assumed that the modification of 3-alkyl-2-thioxo-4*H*-tetrahydroimidazolin-4-one ligands with a redox-active ferrocenyl fragment would allow the synthesis of new classes of Cu(I) or Cu(II/I) coordination compounds with an increased bioavailability, in comparison with non-modified analogs. Thus, the purpose of this work was to synthesize ferrocenyl-containing ligands **5** and **6** and their copper coordination compounds **7** and **8** whose structures are shown below:

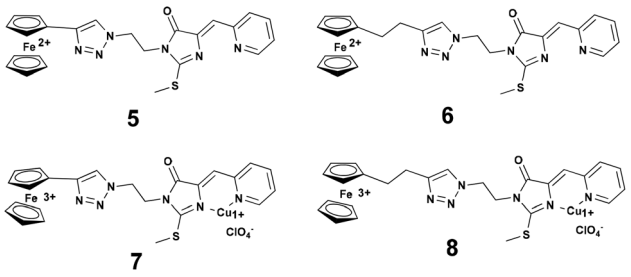

2. Results and discussion

Materials and methods and the details of synthetic procedures for all mentioned substances are given in the ESI (ESI section 1†).

2.1. Synthesis

The synthesis of the target ligands **5** and **6** (Scheme 1) was carried out using a copper-catalyzed azide–alkyne cycloaddition reaction (CuAAC) between the azide-containing imidazol-4-one 2 and the alkynyl-substituted ferrocene derivatives **3** and **4**. 3-Azidoethyl-substituted 2-methylthio-imidazole-4-one was chosen for the insertion of the copper ion chelating fragment into the target ligand molecules. Ethynylferrocene 3 and 4-ferrocenylbutyn-1 4 were used as sources of the ferrocene moiety; these molecules differ by the electronic characteristics of the ferrocene nucleus: for the first compound, cyclopentadienyl, the fragment is linked to the acceptor alkyne substituent, and for the second compound, it is linked to the donor alkyl fragment. It should be noted that very few click reactions with ferrocene derivatives are described in the literature.[28] When the CuAAC reaction conditions were optimized, it was found that in the organic solvents (dichloromethane, acetonitrile, tetrahydrofuran, dimethylformamide) the reactions do not proceed or proceed with the yield not exceeding 5%, and also that the main reaction by-products for the reactions carried out in an aqueous medium are the products of partial and complete hydrolysis of the initial substances, intermediates and target molecules. Thus, in order to achieve optimal yields, it is necessary to minimize the amount of water in the reaction mixture. The optimal conditions for the azide–alkyne cycloaddition reaction were the use of copper(II) sulfate in the presence of a twofold excess of sodium ascorbate in methylene chloride, with the addition of a few drops of water to dissolve inorganic salts (see the experimental part in the ESI†).

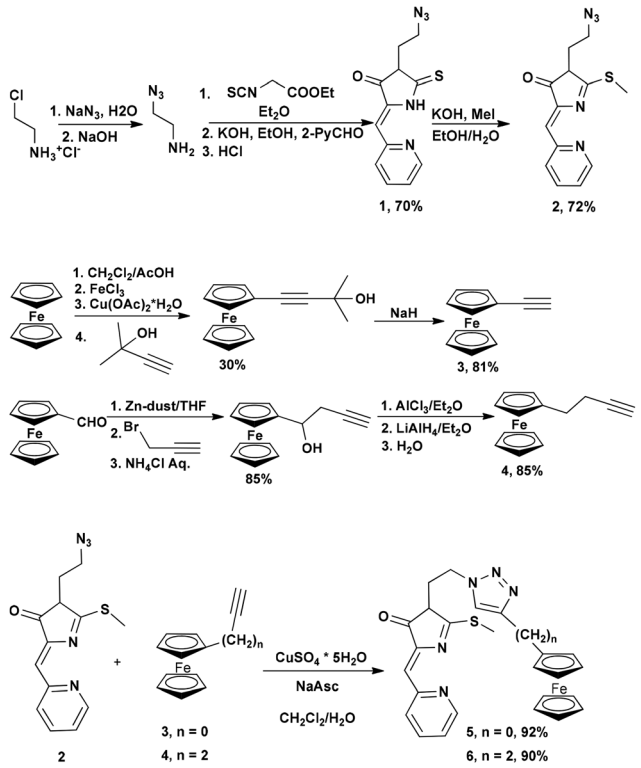

Scheme 1 Synthesis of ferrocene-based ligands **5** and **6**.

Since ligands **5** and **6** contain redox-active ferrocene fragments in their structure, we assumed that they can reduce copper(II) to copper(I) during complexation with copper(II) salts to form ferrocenyl cations. Therefore, it was necessary to avoid carrying out the reaction in the presence of nucleophiles capable of interacting with ferrocenyl cations.

It is known that ferrocenylium-cation $FeCp_2^+$ is stable in acetonitrile, acetone and nitromethane in the absence of strong nucleophiles, but it is decomposed by Cl^- and Br^- (to $FeCp_2$ and $FeHal_4^-$, and in some cases to other products), and also by solvents such as DMF, DMSO, and HMPTA, and nitrogen-containing ligands PHEN and BIPY (to $FeCp_2$ and Fe^{2+} complex, octahedrally coordinated by the molecules of the added ligand).[29] It is believed that in the first stage, the ligand exchange occurs at the Fe^{3+} atom, as a result of which the $C_5H_5^-$ anion is liberated, being the strongest reducing agent and freeing up the formed $FeCp_2^+$ and Fe^{3+} complex to the final products. Since the ligand exchange and reduction reactions occur almost simultaneously, and the transformation of the C_5H_5 radicals is irreversible, in reality the destruction of $FeCp_2^+$ is also possible with nucleophiles that are much weaker than $C_5H_5^-$. Taking this into account, complexation reactions of ligands **5** and **6** with Cu(II) was carried out in acetonitrile, and $Cu(ClO_4)_2$ containing a non-nucleophilic perchlorate anion was chosen as the initial copper salt. The best results of the complexation reactions were obtained by mixing a slurry of an organic ligand in acetonitrile with a solution of copper(II) perchlorate in acetonitrile in a molar ratio of 1 : 1. When mixing the reagents, rapid dissolution of the suspended ligand was observed and the formation of a dark green solution of coordination compound **7** or **8**, the proposed structure of which is shown in Scheme 2. Complexes **7** and **8** were characterized by MALDI and HRMS methods, UV-vis, IR and XANES spectroscopy, as well as using cyclic voltammetry data to determine the oxidation states and local environment of metal ions. Broad bands near 1100 cm^{-1} and a sharp band near 625 cm^{-1} are observed in the IR spectra of the complexes **7** and **8** (Fig. S18 and S20†), which could be due to the antisymmetric stretching and bending of perchlorate ions, respectively. No splitting pattern of the perchlorate peak was observed. This is in favor of the fact that the perchlorate ions are most likely not coordinated with the metal ions and are present in the crystal lattice as counterions.[30,31]

The data of reaction mixture monitoring by CV, UV-vis and EPR spectroscopy show that the process of complexation precedes the reduction of copper and the end of the complexation and the beginning of the oxidation–reduction reaction occur within a time of ~1 min from the mixing of the starting compounds (section 2.2). The kinetics of the oxidation–reduction process in the bimetallic "Fe^{2+}–Cu^{2+}" redox system was studied in more detail by EPR (section 2.4) with the example of the ligand **6** and $CuCl_2 \cdot 2H_2O$ interaction.

Thus, bimetallic coordination compounds Fe^{3+}/Cu^+ of a previously unknown structural type have been synthesized. At the moment, as far as we know, only coordination compounds of ferrocene derivatives with Cu(II) or Cu(I) in which intramolecular redox processes do not occur are described in the literature.[32,33] In contrast, the ferrocene-containing organic ligands **5** and **6** described in this work in the complexation reactions efficiently reduce the coordinated copper(II) ions and stabilize them in the valence state (+1).

2.2 Cyclic voltammetry

Ligands **5** and **6** were investigated by cyclic voltammetry (CV) and rotating disk electrode (RDE) techniques in DMF and CH_3CN solutions on a glassy carbon electrode in the presence of 0.1 M Bu_4NClO_4 as an indifferent electrolyte. The obtained results are summarized in Table 1.

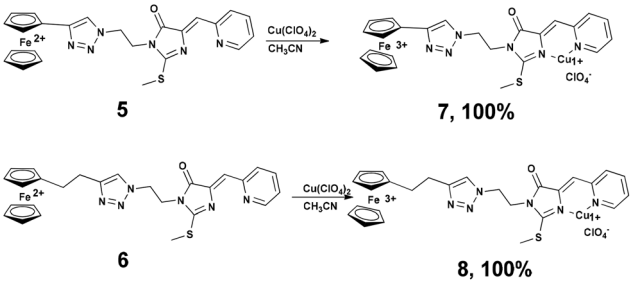

Scheme 2 Synthesis of complexes **7** and **8**.

Table 1 Electrochemical potentials (*vs.* Ag/AgCl/KCl (aq. sat.)) of inorganic copper salts, ligands **5** and **6** and their copper complexes in CH_3CN or DMF (0.1 M Bu_4NClO_4, glass-carbon electrode; potential scan rate 100 mV s^{-1})

Compound	Solvent	E_{pc}, B	E_{pa}, B
$Cu(CH_3CN)_4ClO_4$	CH_3CN	−0.85/−0.42, −0.13 (desorption)	1.16/1.06
$Cu(ClO_4)_2{\cdot}6\,H_2O$	CH_3CN	1.03/1.11 −0.68/−0.42, −0.19 (desorption)	—
$CuCl_2{\cdot}2\,H_2O$	DMF	0.11/1.23 −0.21	0.95
5	CH_3CN	−1.28 −1.88 −2.01	0.52/0.47 1.24 1.68 1.85
6	CH_3CN	1.30 −1.78	0.44/0.39 0.87 1.44 1.70
7	CH_3CN	−0.47 −0.85/−0.17 (desorption)	0.54/0.47 1.56
8	CH_3CN	−0.48 −1.13/−0.04 (desorption)	0.46/0.39 1.34
9	DMF	−0.76 −1.26/−1.23	0.54/0.46

The oxidation of ligand **6** containing the donor alkyl substituent in the cyclopentadienyl ring proceeds reversibly at $E_{1/2}$ = 0.42 V (CH_3CN) over the ferrocene (Fc) fragment. Ligand **5** oxidizes at a higher potential ($E_{1/2}$ = 0.50 V), which is apparently due to the accepting nature of the triazole moiety conjugated to the cyclopentadienyl ring. The first stage of the reduction of ligands **5** and **6** at E = 1.28–1.30 V occurs irreversibly, apparently, over the conjugated pyridylmethyleneimidazolinone fragment, as was previously observed for ligands, derivatives of 2-thiohidantoin.[34,35]

The addition of Cu(II) salts ($CuCl_2{\cdot}2H_2O$ or $Cu(ClO_4)_2{\cdot}6H_2O$) to an electrochemical cell, containing a solution of ligand **5** or **6**, leads to significant changes in CV. In all cases, oxidation of the ferrocene fragment to the ferrocenyl cation and the reduction of Cu^{2+} to Cu^{1+} occur. The formation of the ferrocenyl cation is indicated by a change in the color of the solution from light yellow (the color of the initial ligand) to blue-green (the characteristic color of the ferrocenyl cation,[36] Fig. S1†) instantaneously or for several minutes, as well as by the characteristic changes in RDE: the current of Fc^+/Fc becomes cathodic (Fig. S2†), which corresponds to the reduction process.

For complex **7**, forming from the ligand **5**, according to the CV data, $Cu^+ \rightarrow Cu^0$ reduction occurs at −0.85 V, and the subsequent reduction peaks of the ligand fragment (E = −1.13 V) are shifted to the anode potential region (Fig. S3†). But when the ligand **6** was mixed with $Cu^{II}(ClO_4)_2$ in CH_3CN, on the first scans of the CV curves in the reduction region, there are two peaks corresponding to the $Cu^+ \rightarrow Cu^0$ transitions at −0.48 V and −0.85 V, which indicates the formation of two different coordination compounds in the solution and is consistent with the EPR data (see section 2.4). The second peak disappears after a few minutes; the intensity of the peak at −0.48 V, related to the copper(I)-containing complex, in contrast increases. In addition, the reduction of the ligand fragment (E = −1.13 V) is facilitated by 270 mV compared with the free ligand (Fig. 1). These changes indicate the formation of complex **8**, with the assumed structure shown in Scheme 2.

Thus, ligand **6** with a linker between the ferrocene fragment and the triazole ring, according to the CV, forms an ultimate copper complex more slowly than ligand **5**, in which ferrocene and triazole are directly linked. In addition, in the case of ligand **6**, it is possible to affirm the existence in CH_3CN solution of an intermediate copper-containing compound that turns into complex **8**.

When the ligand **6** reacts with $Cu^{II}Cl_2{\cdot}2H_2O$ in DMF poorly soluble copper(I) salt (possibly $Cu^{I}Cl$) apparently forms and precipitates on the surface of the electrode, since only low intense peaks are observed in the reduction region in the CV besides the $Fc^+ \rightarrow Fc$ reduction peak (Fig. S4†). Apparently, in the presence of chloride anions, the formed Fc^+ is unstable and decays, with the loss of iron, as described in ref. 37. Thus, in this case, the ligand **6** and copper salt interaction seems to proceed according to the sequence:

$$\mathbf{6} + Cu^{II}Cl_2 \rightarrow Cu^{I}Cl + \mathbf{6}^+ \rightarrow \text{products of } \mathbf{6}^+ \text{ decomposition.}$$

The interaction of ligand **5** with $Cu^{II}Cl_2{\cdot}2H_2O$ in DMF takes place slowly; in contrast to all the other reactions studied, this process is the only reaction with Cu(II) salts, where the color change of the solution to blue-green occurs in 10–15 minutes at room temperature. The complete disappearance of the $Cu^{2+} \rightarrow Cu^+$ peak occurs only after ~1.5 hours after the mixing of the ligand and the salt. Thus, the reaction

$$\mathbf{5} + Cu^{II}Cl_2 \rightarrow [\mathbf{5}^{\pm}]Cu^{I}Cl.$$

in this case is slow. Note also that based on the results of the electrochemical study the copper(II) reduction steps follow its coordination with the ligand (Scheme 3); this is evidenced

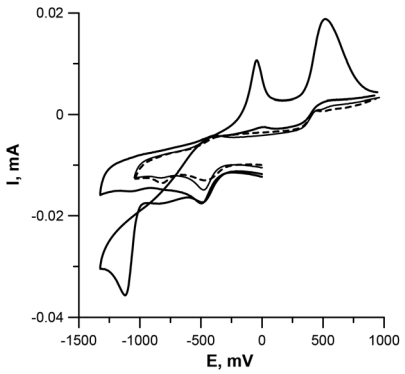

Fig. 1 CV curves of a ligand **6** mixture with $CuII(ClO_4)_2{\cdot}6H_2O$ (solid) and the first CV curve after **6** and $CuII(ClO_4)_2{\cdot}6H_2O$ were mixed (dotted line) in CH_3CN (10^{-4} M, GC electrode, 0.1 M Bu_4NClO_4).

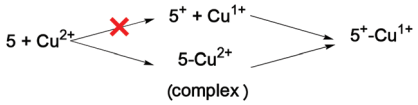

Scheme 3 The sequence of reduction and coordination of the copper (II) ion by the ligand **5** based on the CV data.

by the absence of any peaks of the Cu(I) derivative reduction in the voltammogram, except for the peaks of the final complex.

Note that for all the processes described in this section, a catalytic increase in the oxidation current Fc → Fc^+ was observed on the reverse CV scans (Fig. 1 and S2–S4†), which can be explained by the participation of the regenerated Cu^{2+} in the oxidation of ferrocene fragments (Fc → Fc^+), which are at these potentials in an electrochemically reduced state.

Thus, similar values of ferrocene fragment oxidation potentials and Cu^{II} reduction potentials make it possible for electronic transition from the HOMO Fc to the LUMO Cu(II), which confirms the hypothesis that the organic ligands **5** and **6** are able to effectively stabilize Cu(I) ions. Furthermore, the stage of formation of the copper(II) complex with the ferrocene-based ligand precedes the stage of Cu(II) → Cu(I) reduction.

2.3 XANES spectroscopy

For the coordination compound **7**, XANES absorption spectra for iron and copper were recorded. Comparing the XANES spectrum of the K-edge of copper for this sample with the spectra of the reference samples (Fig. 2, top), we can conclude that there is a similarity in the local copper environment of the investigated complex and copper(II) nitrate. However, in the absorption edge region, the spectrum of complex **7** has an appreciable feature, which is caused by the presence of Cu^{1+} ions in the sample. It shoud be noted, that compound **7** gradually oxidized by air oxygen forming the copper(II) derivative if it is stored without an argon atmosphere.

By analyzing the XANES spectrum behind the K-edge of the iron for this sample (Fig. 2, bottom), it can be seen that the experimental curve lies between the spectra of the standard reference samples. Despite the fact that Fe^{2+} ions are present in the sample with high probability, the presence of Fe^{3+} is also evident.

Thus, in view of the presence of Fe(III) ions and Cu(II) ions in the sample of the coordination compound **7**, it can be concluded that even in a solid sample an oxidation–reduction process $Fe^{2+} + Cu^{2+} \Leftrightarrow Fe^{3+} + Cu^{1+}$ discussed in sections 2.1 and 2.2 takes place. Also, it can be assumed that the oxidation of Cu(I) ions by the oxygen of the air leads to the observed result. However, we assumed that under the reducing conditions of the cellular environment this process will not occur.

2.4 Kinetic studies of complexation and redox transformations by EPR spectroscopy

To confirm the presence of the redox-processes with the participation of ferrocene electronic switches and coordinated

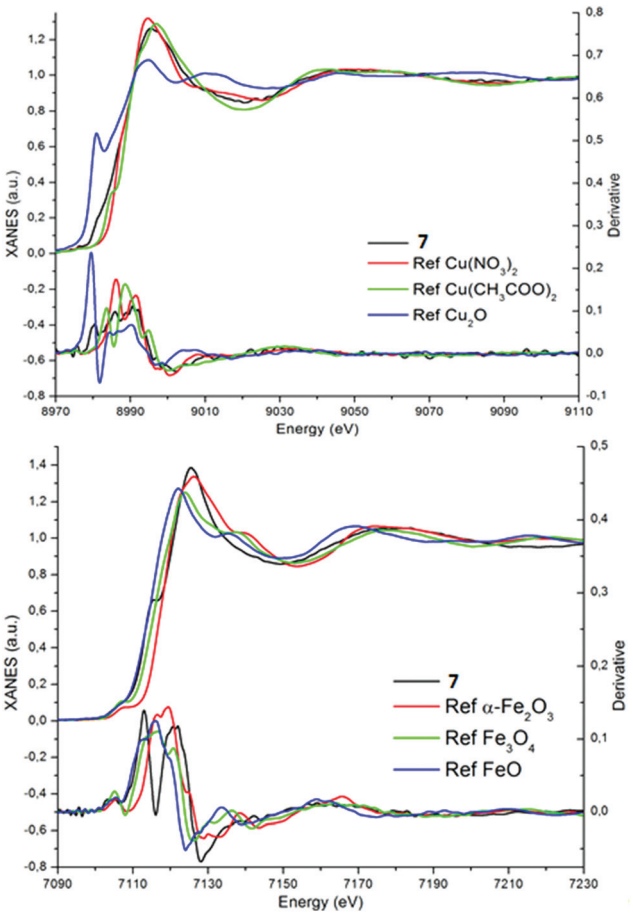

Fig. 2 XANES spectra and their first derivatives behind the K-edge of copper for the sample of complex **7** and reference compounds $Cu(NO_3)_2$, $Cu(CH_3COO)_2$ and Cu_2O (top) and α-Fe_2O_3, Fe_3O_4, and FeO (bottom).

copper ions, we investigated the kinetics of redox reactions. As soon as paramagnetic copper(II) ions are converted to diamagnetic copper(I), electron-paramagnetic resonance spectroscopy (EPR) was used.

EPR has several advantages that are significant in the framework of this study, it gives additional structural information on the symmetry of copper(II) ions' coordination environment.

Based on the cyclic voltammetry data (section 2.2), the reaction of ligand **6** with $Cu^{II}Cl_2$ in DMF was chosen to study the kinetics of the process due to the long enough reaction time span.

A comparison of the EPR spectra of a mixture of ligand **6** with copper chloride dehydrate (Fig. 3) shows that the integral intensity of paramagnetic Cu^{2+} ions expectedly gradually decreases.

At the same time, the shape of the EPR spectrum does not change with time, meaning that the complexation occurs immediately after mixing the ligand with copper chloride solution, before registration of the first EPR spectrum (Scheme 3).

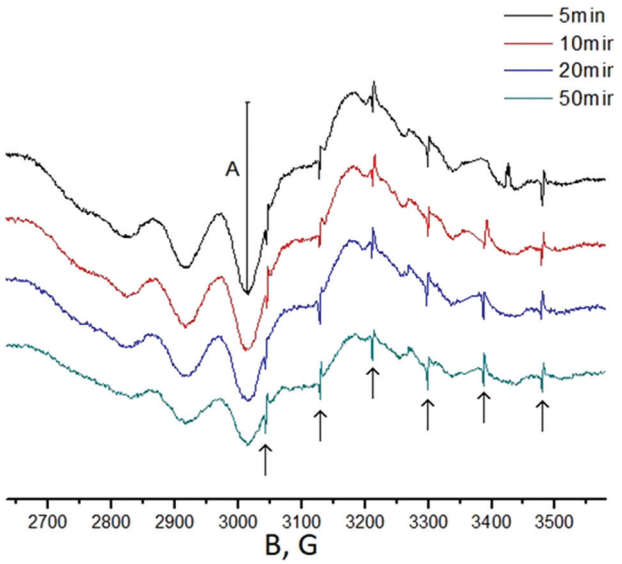

Fig. 3 **6** with an equivalent amount of copper(II) chloride dihydrate in DMF over time. The arrows indicate the position of the components of the hyperfine structure of the diamagnetically diluted solution of Mn^{2+} ions in MgO (the internal standard for the value of the magnetic field induction).

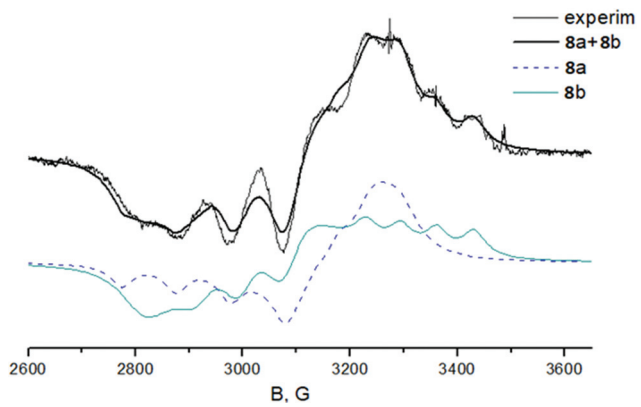

Fig. 4 The experimental EPR spectrum of the solution of coordination compound **8**, and the simulated EPR spectra of isomeric coordination compounds **8a** (pyramidal copper surroundings) and **8b** (octahedral copper surroundings).

The experimental EPR spectra (Fig. 4) correlate with the sum of the simulated spectra for the octahedrally coordinated isomer **8a** (~40%) and the square pyramidally coordinated isomer **8b** (~60%). The proposed structure of the isomeric complexes is shown in Scheme 4.

The kinetic curves of Cu^{2+} ion concentration (C) decrease and its evolution (concentration *vs.* square root of reaction time) are shown in Fig. 5. It should be noted that in some cases this dependence is characteristic of diffusion-controlled processes.

The redox reactivity of **8a** and **8b** cannot be correctly estimated in the presence of compound **6**, as individual concentrations of **8a** and **8b** are associated with large errors introduced in the simulated EPR spectra.

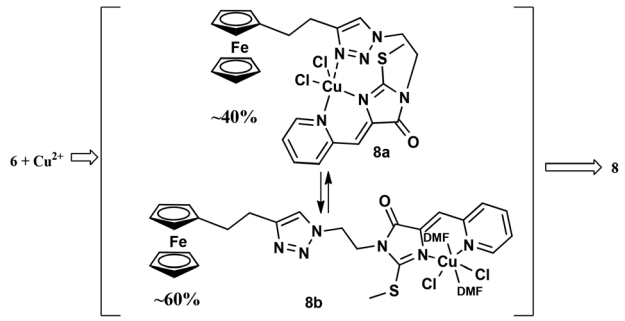

Scheme 4 The proposed paths of the complex **8** formation (based on the EPR data).

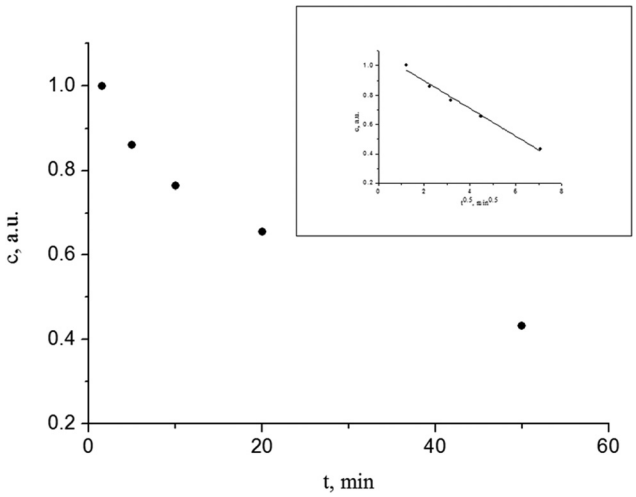

Fig. 5 The kinetic curve corresponding to the consumption of paramagnetic Cu^{2+} ions during the redox process in the solution of compound **6** and its processing in coordinates $C-t^{1/2}$.

EPR spectra do not undergo fundamental changes during the redox process, meaning that there is an equilibrium between isomers **8a** and **8b** in the reaction mixture.

Based on the EPR data, we can propose a hypothesis that two isomeric intermediate copper(II) complexes **8a** and **8b** with different coordination environments exist in the solution and then both are converted into complex **8**.

2.5 *In vitro* biological studies

2.5.1 MTT assay. The MTT assay was conducted on MCF-7 (human breast adenocarcinoma cell line), A549 (human lung carcinoma), HEK293 (human embryonic kidney), and VA13 (fissile lung fetal cells) cell lines in accordance with the standard MTT method with three repeats for averaging the results. CC_{50} values of compounds **7** and **8** and the corresponding ligands **5** and **6** were compared to determine the role of copper ions in toxicity. The cytotoxicity data for compounds **5–8** are

Table 2 Cytotoxicity of compounds **3–6** compared to that of doxorubicin and cisplatin

Compound	CC_{50} HEK293	CC_{50} MCF7	CC_{50} A549	CC_{50} Va-13
5, μM	>	>	>	>
6, μM	~3	~11	5.5 ± 0.4	11 ± 2
7, μM	16 ± 2	17.7 ± 2	28.1 ± 2.4	21.1 ± 1.8
8, μM	28.7 ± 3.5	~33	54.7 ± 7	42.7 ± 2.7
Doxorubicin, nM	11.5 ± 3.2	55.4 ± 11.8	47.9 ± 7.9	159.9 ± 27.4
Cisplatin, μM (ref. 17)	12.4 ± 3.9	64.1 ± 3.9	>30	2.9 ± 0.3

Table 3 Concentration stability constants of conjugates of coordination compounds **5** and **6** with bovine serum albumin, literature data for doxorubicin are given for comparison

Coordination compound	K_{app} (BSA)	Number of binding sites
5	$(1.47 \pm 0.04) \times 10^4$	0.98
6	$(4.5 \pm 0.3) \times 10^5$	1.15
7	$(4.85 \pm 0.05) \times 10^5$	1.16
8	$(9.2 \pm 0.5) \times 10^1$	0.54
Doxorubicin	$(7.8 \pm 0.7) \times 10^3$	—

given in Table 2. All the tested derivatives have a cytotoxicity comparable to or higher than cisplatin and doxorubicin.

Ferrocene derivative **6a** exhibits a noticeable cytotoxicity. The introduction of a $(CH_2)_2$ linker between the ferrocene and triazole moieties of the ligand leads to a cytotoxicity increase, as seen from the cytotoxicity of compounds **5** and **6**. Typically, the cytotoxicity of metal–thiohydantoin complexes is defined by a metal.[38] Surprisingly, the introduction of the copper ion into the ferrocene ligand **6** results in cytotoxicity reduction, which we associate with the planar molecular geometry change and, consequently, its inability to bind to the target in the cell.

2.5.2 BSA binding. The interaction between transport proteins and various drugs is crucial for a wide range of pharmacological, biological, and clinical applications.[39] The understanding of the binding of drugs to serum albumin *in vitro* can help in providing guidelines for rational drug design.[40] Serum albumin is the most abundant of the proteins in blood plasma, and it serves as a transport protein for drugs.

For the investigation of the BSA binding ability of **7** and **8** and predicting their stability under physiological conditions of the blood, a standard experiment using fluorescence quenching was used.

Fig. S6 and S7† show the plots of fluorescence quenching of bovine serum albumin in response to an increasing concentration of compounds **7** and **8**. The steady decrease in the intensity of fluorescence in response to an increase in the concentration of coordination compounds allows us to conclude that all of the tested compounds bind to bovine serum albumin. To quantify the binding by the Sketchard method, the obtained dependences of the decrease in fluorescence intensity on the concentration of coordination compounds were linearized in double inverse logarithmic coordinates. The linear graphs of dependencies by Sketchard are presented in Fig. S7 in the ESI.†

The obtained values are shown in Table 3. The number of binding sites and constants, measured in the experiment, is well consistent with the values obtained earlier for analogous copper coordination compounds and the literature data[41] that one copper binding site is present in the molecules of bovine and human serum albumin. Thus, compounds **5–7** have sufficiently good affinities for BSA and can be transported through the bloodstream due to the interaction with blood transport proteins.[39,42]

2.5.3 Inhibition of telomerase activity. Since the first years of telomerase research, the enzyme has been considered a universal target for anticancer therapy. Recent studies have also considered the telomerase activity as an important potential target in drug development and anti-cancer therapy.[43]

Earlier, we have described[16] the coordination compounds of copper(II,I) based on 2-alkylthioimidazolin-4-ones with promising cytotoxicity, wherein the mechanism of cytotoxic action was associated with the inhibition of telomerase activity. In this research work, we have designed new Cu(I)/Fe(III) coordination compounds with a pronounced cytotoxic activity against tumor cells (section 2.5.1). It was assumed that the cytotoxic activity of the ferrocene-containing ligands **5** and **6** and binuclear Cu(I)/Fe(III) coordination compounds **7** and **8** could also be due to the inhibition of telomerase activity. The effects of compounds **5–8** (20/200 μM) and BIBR (50 μM) on the telomerase activity from HEK293 T cells were evaluated *via* RQ-TRAP.

In the case of the classical inhibitor of telomerase activity, BIBR (50 μm), the telomerase activity is only reduced when the inhibitor is added to the telomerase reaction, and in the case of the inhibitor addition after the reaction, the telomerase activity persists before PCR. The data obtained for ligands **5** and **6** and coordination compounds **7** and **8** show that only ligand **6** exhibits a significant inhibition of telomerase activity (35 ± 19% telomerase activity and 89 ± 51% PCR control in the presence of 20 μM of **6**; see Fig. S8 in the ESI†). It is important to note that the ability to inhibit the telomerase enzyme is correlated with cytotoxicity; reducing the length of the linker and introducing a copper ion into the ferrocene ligand **6** reduce the ability to inhibit the telomerase enzyme and cytotoxicity, respectively.

Hereby, we have designed a ferrocene-containing cytotoxic agent, which is a ferrocene-containing conjugate of 2-alkylthioimidazolin-4-one.

2.5.4 DNA cleavage assay. We have studied the ability of compounds **7** and **8** to intercalate DNA with fluorescence emission using ethidium bromide and have shown that both the complexes are not DNA intercalators (see the ESI†).

The half-life of DNA by spontaneous hydrolysis will be thousands to billions of years.[44] However, it could be hydrolyzed with the help of artificial nucleases or be damaged by reactive oxygen species (ROS). Many transition metal complexes were used as DNA cleavage agents. The coordination compounds of

Table 4 The results of pUC18 DNA cleavage catalyzed by 0.250 mM of different cleavage agents for 4 h

Cleavage agent	LC DNA (%)	NC DNA (%)	SC DNA (%)
$CuCl_2$	0	25	75
Control (without treatment)	7	1	92
5	18	18	64
6	5	31	64
7	9	75	16
8	8	60	32

copper with nuclease activity are widely described.[45] Due to the biologically accessible redox potential, Cu complexes belong to the most frequently studied artificial metallonucleases. We have investigated the nuclease activity of compounds **5–8** on the substrate, supercoiled pUC18 plasmid DNA, by gel electrophoresis on agarose. The DNA cleavage ability was obtained from the conversion amount of supercoiled DNA (SC) to nicked circular form (NC) and linearized DNA (LC).

To be sure of the nuclease active point in ferrocene-containing ligands **5** and **6** or coordination compounds **7** and **8**, the cleavage reaction catalyzed by compounds **5–8** was compared with those reactions catalyzed by an equimolar amount of $CuCl_2$.

Table 5 Cytosol/pellet distribution of coordination compounds **7** and **8** investigated by the AAS method

		Cytosol	Pellet
7	% of the dose added to the cells	11.18 ± 2.65	3.45 ± 0.61
	% of the amount of the drug penetrated into the cell	75.92 ± 7.53	24.08 ± 7.53
8	% of the dose added to the cells	11.10 ± 0.23	15.68 ± 5.79
	% of the amount of the drug penetrated into the cell	42.44 ± 9.67	57.56 ± 9.67

Table 6 The results of apoptosis test catalyzed by ligand **6** and coordination compound **8**

	C, μM	%, apoptotic cells
8	50	15.9
8	100	19.4
6	5	33.1
6	20	43.4
DMSO		16.6

The results are presented in Table 4 and in Fig. S8.† The nuclease activity of complexes **7** and **8** was not the simple summation of the activities of free ligands **5** and **6** and copper(II) salt.

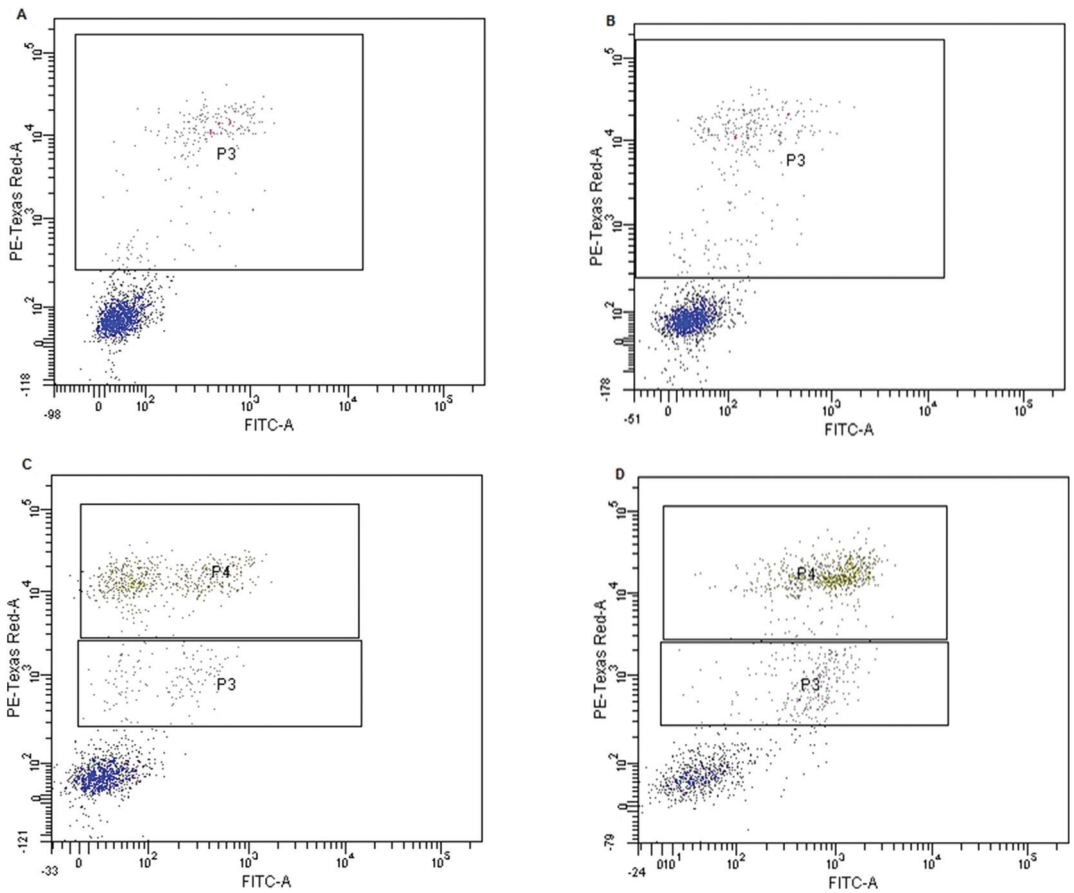

Fig. 6 Flow cytometry analysis in A549 cells after ligand **6** and complex **8** treatment. A549 cells treated with 50 μM of complex **8** (A), 100 μM of complex **8** (B), 5 μM of ligand **6** (C) and 20 μM of ligand **6** (D).

The addition of increasing amounts of ligands **5** and **6** to pUC18 DNA does not lead to a significant change in the DNA pattern. In the case of the attachment to the equimolar amount of DNA of the coordination compounds **7** and **8**, multiple double-stranded DNA breaks are observed. Thus, Cu(I),(I) ions play an important role in the scission ability of the complexes.

2.5.5 Cytosol/pellet distribution investigated by AAS. This work is devoted to the development of high-permeability drugs that can effectively overcome the cell membrane. We have investigated the cytosol/pellet distribution of coordination compounds **7** and **8**. Mammary carcinoma cells 4T1 were incubated with coordination compounds **7** and **8**, and the accumulation of copper in the pellet and cytosol was determined by atomic adsorption spectroscopy (AAS). The results are presented in Table 5.

Cellular accumulation alone is insufficient to enable any activity; any potential therapeutic agent must also be able to reach its target within the cell. As can be seen from the data obtained, the length of the linker significantly affects the ability of the coordination compound to accumulate in pellet. The coordination compound **8** has a lower cytotoxicity than its analogue **7**, however, it is predominantly localized in the pellet, which provides the possibility of its effect on DNA-operating enzymes, DNA cleavage and mitochondria.

2.5.6 Flow cytometry-based apoptosis detection. Apoptosis is a form of programmed cell death that results in the orderly and efficient removal of damaged cells, such as those resulting from DNA damage or during development. Apoptosis can be triggered by signals from within the cell, such as genotoxic stress, or by extrinsic signals, such as the binding of ligands to cell surface death receptors.[46] The cytotoxic activity of a large number of antitumor drugs occurs due to cellular apoptosis.[47,48] In order to test whether the cytotoxic activity of ligand **6** and copper-containing complex **8** is based on the induction of cell apoptosis, flow cytometry using the FITC Annexin V Apoptosis Detection Kit protocol was conducted. A549 cells were incubated with the investigated compounds **6** and **8** for 24 h. The results are presented in Table 6. The populations P3 and P4 show the percentage of apoptotic cells (double positive cells). The treatment of cells with ligand **6** (Fig. 6C and D) results in the accumulation of two populations of apoptotic cells with different efficiencies of PI-staining. The intensity of PI-staining demonstrates the phase of apoptosis: more intensive staining corresponds to the late phase.

As can be seen from the data obtained, ligand **6** induces cell death along the apoptotic pathway. Unlikethis, the coordination compound **8**, even at concentrations an order of magnitude greater than the ligand, does not show traces of early apoptosis. Since the ability to cause apoptosis correlates with the cytotoxicity data, it can be assumed that the antitumor activity of ligand **6** is associated with apoptotic cell death.

3. Conclusions

In conclusion, the ferrocene-containing derivatives of 2-thiohydantoins were firstly synthesized as redox active ligands for studying their interaction with copper salts. The possibility of the intramolecular redox reaction of the obtained ferrocene-substituted imidazolones with copper(II) chloride and perchlorate has been shown. The preliminary *in vitro* biological studies of the obtained ferrocene-substituted ligands and their Fe, Cu-containing coordination compounds were carried out.

Author contributions

D. A. Guk, N. S. Dashkova, O. Krasnovskaya, V. P. Dyadchenko, E. S. Yudina, M. A. Kosarev – synthesis of ligands and complexes. D. A. Skvortsov, M. P. Rubcova, A. S. Semkina, K. Y. Vlasova, R. R. Shafikov, A. A. Andreeva – biological research. V. I. Pergushov, M. Ya. Melnikov – EPR spectroscopy. A. V. Soldatov, V. V. Shapovalov – XANES spectroscopy. N. V. Zyk, A. G. Majouga, E. K. Beloglazkina – spectral studies, preparation of an article for publication.

Conflicts of interest

There are no conflicts of interest to declare.

Acknowledgements

The authors are thankful to Thermo Fisher Scientific Inc., Textronica AG group (Moscow, Russia), and personally to Prof. Alexander Makarov for providing the Orbitrap Elite mass spectrometer for this work. This work in part of NMR study was supported by the M.V. Lomonosov Moscow State University Program of Development. We are grateful to the Russian Foundation of Basic Research (Projects 16-03-00921 and 18-29-08060) for financial support.

Notes and references

1 G. J. Dougbartey, L. J. Peppone and I. A. de Graaf, *Toxicol.*, 2016, **371**, 58–66.
2 J. Kuduk-Jaworska and J. J. Jański, *J. Inorg. Biochem.*, 2017, **170**, 148–159.
3 C. R. Munteanu and K. Suntharalingam, *Dalton Trans.*, 2015, **44**(31), 13796–13808.
4 J.-X. Liang and H.-J. Zhong, *J. Inorg. Biochem.*, 2017, **177**, 276–286.
5 M. Chikira, C. Hee Ng and M. Palaniandavar, *Int. J. Mol. Sci.*, 2015, **16**, 22754–22780.
6 C. Santini, M. Pellei, V. Gandin, M. Porchia, F. Tisato and C. Marzano, *Chem. Rev.*, 2014, **114**, 815–862.
7 H. W. Kuo, S. F. Chen, C. C. Wu, D. R. Chen and J. H. Lee, *Biol. Trace Elem. Res.*, 2002, **89**(1), 1–11.
8 S. L. Rizk and H. H. Sky-Peck, *Cancer Res.*, 1984, **44**(11), 5390–5394.
9 F. K. Habib, T. C. Dembinski and S. R. Stitch, *Clin. Chim. Acta*, 1980, **104**(3), 329–335.

10 S. B. Nayak, V. R. Bhat, D. Upadhyay and S. L. Udupa, *Indian J. Physiol. Pharmacol.*, 2003, **47**(1), 108–110.
11 M. Díez, M. Arroyo, F. J. Cerdàn, M. Muñoz, M. A. Martin and J. L. Balibrea, *Oncology*, 1989, **46**(4), 230–234.
12 D. C. Brady, M. S. Crowe, M. L. Turski, G. A. Hobbs, X. Yao, A. Chaikuad, S. Knapp, K. Xiao, S. L. Campbell, D. J. Thiele and C. M. Counter, *Nature*, 2014, **509**, 492–496.
13 P. Sathyadevi, P. Krishnamoorthy, R. R. Butorac, A. H. Cowley and N. Dharmaraj, *Metallomics*, 2012, **4**, 498–511.
14 M. Chikira, C. Hee Ng and M. Palaniandavar, *Int. J. Mol. Sci.*, 2015, **16**, 22754–22780.
15 C. E. Paulsen and K. S. Carroll, *Chem. Rev.*, 2013, **113**, 4633–4679.
16 A. G. Majouga, M. I. Zvereva, M. P. Rubtsova, D. A. Skvortsov, A. V. Mironov, D. M. Azhibek, O. O. Krasnovskaya, V. M. Gerasimov, A. V. Udina, N. I. Vorozhtsov, E. K. Beloglazkina, A. Leonid, L. V. Mikhina, A. V. Tretyakova, N. V. Zyk, N. S. Zefirov, A. V. Kabanov and O. A. Dontsova, *J. Med. Chem.*, 2014, **57**, 6252–6258.
17 K. Tishchenko, E. Beloglazkina, M. Proskurnin, V. Malinnikov, D. Guk, M. Muratova, O. Krasnovskaya, A. Udina, D. Skvortsov, R. R. Shafikov, Y. Ivanenkov, V. Aladinskiy, I. Sorokin, O. Gromov, A. Majouga and N. Zyk, *J. Inorg. Biochem.*, 2017, **175**, 190–197.
18 E. K. Beloglazkina, O. O. Krasnovskaya, D. A. Guk, V. A. Tafeenko, A. A. Moiseeva, N. V. Zyk and A. G. Majouga, *Polyhedron*, 2018, **148**, 129–137.
19 D. X. West and A. E. Liberta, *Coord. Chem. Rev.*, 1993, **123**, 49–71.
20 Á Mooney, A. J. Corry, C. N. Ruairc, T. Mahgoub, D. O'Sullivan, N. O'Donovan, J. Crown, S. Varughese, S. M. Draper and D. K. Rai, *Dalton Trans.*, 2010, **39**, 8228–8239.
21 B. Long, S. Liang, D. Xin, Y. Yang and J. Xiang, *Eur. J. Med. Chem.*, 2009, **44**, 2572–2576.
22 L. V. Snegur, Y. S. Nekrasov, N. S. Sergeeva, Z. V. Zhilina, V. V. Gumenyuk, Z. A. Starikova, A. A. Simenel, N. B. Morozova, I. K. Sviridova and V. N. Babin, *Appl. Organomet. Chem.*, 2008, **22**, 139–147.
23 A. P. Ferreira, J. L. F. da Silva, M. T. Duarte, M. F. M. da Piedade, M. P. Robalo, S. G. Harjivan, C. Marzano, V. Gandin and M. M. Marques, *Organometallics*, 2009, **28**, 5412–5423.
24 R. A. Hussain, A. Badshah, J. M. Pezzuto, N. Ahmed, T. P. Kondratyuk and E.-J. Park, *J. Photochem. Photobiol., B*, 2015, **148**, 197–208.
25 R. Schobert, S. Knauer, S. Seibt and B. Biersack, *Curr. Med. Chem.*, 2011, **18**, 790–807.
26 A. Nguyen, S. Top, A. Vessieres, P. Pigeon, M. Huche, E. A. Hillard and G. Jaouen, *J. Organomet. Chem.*, 2007, **692**, 1219–1225; D. R. K. Weerasuriya, W. P. S. L. Wijesinghe and R. M. G. Rajapakse, *Mater. Sci. Eng.*, 2017, **71**, 206–213.
27 T. K. Goswami, S. Gadadhar, B. Gole, A. A. Karande and A. R. Chakravarty, *Eur. J. Med. Chem.*, 2013, **63**, 800–810.
28 R. Prins, A. R. Korswagen and A. G. T. G. Kortbeek, *J. Organomet. Chem.*, 1972, **39**, 335–344.
29 M. Zábranský, L. Kolářová, I. Císařová and P. Štěpnička, *J. Organomet. Chem.*, 2017, **846**, 217–222.
30 S. Anbu, S. Kamalraj, B. Varghese, J. Muthumary and M. Kandaswamy, *Inorg. Chem.*, 2012, **51**, 5580–5592.
31 S. Anbu, M. Kandaswamy, P. Sathya Moorthy, M. Balasubramanian and M. N. Ponnuswamy, *Polyhedron*, 2009, **28**, 49–56.
32 M. Shabbir, Z. Akhter, I. Ahmad, S. Ahmed, M. Bolte, H. Ismail and B. Mirza, *Inorg. Chim. Acta*, 2017, **463**, 102–111.
33 E. K. Beloglazkina, A. G. Majouga, A. A. Moiseeva, M. G. Tsepkov and N. V. Zyk, *Russ. Chem. Bull.*, 2007, **56**(2), 351–355.
34 A. G. Majouga, E. K. Beloglazkina, A. A. Moiseeva, O. V. Shilova, E. A. Manzheliy, M. A. Lebedeva, E. S. Davies, A. N. Khlobystov and N. V. Zyk, *Dalton Trans.*, 2013, **42**, 6290–6293.
35 M. Cuartero, R. G. Acres, J. Bradley, Z. Jarolimova, L. Wang, E. Bakker, G. A. Crespo and R. De Marco, *Electrochim. Acta*, 2017, **238**, 357–367.
36 P. Zanello, G. Opromolla, L. Pardi, K. H. Pannell and H. K. Sharma, *J. Organomet. Chem.*, 1993, **450**, 193–196.
37 O. O. Krasnovskaya, Y. V. Fedorov, V. M. Gerasimov, D. A. Skvortsov, A. A. Moiseeva, A. V. Mironov, E. K. Beloglazkina, N. V. Zyk and A. G. Majouga, *Arabian J. Chem.*, 2016, DOI: 10.1016/j.arabjc.2016.04.013.
38 A. G. Majouga, E. K. Beloglazkina, A. A. Moiseeva, O. V. Shilova, E. A. Manzheliy, M. A. Lebedeva, E. S. Davies, A. N. Khlobystov and N. V. Zyk, *Dalton Trans.*, 2013, **42**, 6290–6293.
39 S. Sangeetha and M. Murali, *Int. J. Biol. Macromol.*, 2018, **107**, 2501–2511.
40 Y. Kawasaki and E. Friere, *Drug Discovery Today*, 2011, **16**(21–22), 985–990.
41 M. Anjomshoa, M. Torkzadeh-Mahani, J. Janczak, C. Rizzoli, M. Sahihi, F. Ataei and M. Dehkhodaei, *Polyhedron*, 2016, **119**, 23–38.
42 D. Agudelo, P. Bourassa, J. Bruneau, G. Bérubé, É Asselin, H.-A. Tajmir-Riahi and D. S. Sem, *PLoS One*, 2012, **7**, 8.
43 Q. Qi-Pin, M. Ting, T. Ming-Xiong, L. Yan-Cheng and L. Hong, *Eur. J. Med. Chem.*, 2018, **143**, 1597–1603.
44 G. K. Schroeder, C. Lad, P. Wyman, N. H. Williams and R. Wolfenden, *Proc. Natl. Acad. Sci. U. S. A.*, 2006, **103**, 4052–4055.
45 H. Yu, L. Qiao-Sen, Z. Ji, Z. Zhong-Wei and Y. Xiao-Qi, *Bioorg. Med. Chem.*, 2008, **16**(3), 1103–1110.
46 G. Pistritto, D. Trisciuoglio, C. Ceci, A. Garufi and G. D'Orazi, *Aging*, 2016, **8**(4), 603–619.
47 R. S. Y. Wong, *J. Exp. Clin. Cancer Res.*, 2011, **30**(87), DOI: 10.1186/1756-9966-30-87.
48 J. B. Foo, M. L. Low, J. H. Lim, Y. Z. Lor, A. R. Zainol, V. Eh Dam, N. Abdul Rahman, C. Y. Beh, L. C. Chan, C. W. How, Y. S. Tor and L. Saiful Yazan, *BioMetals*, 2018, **31**(4), 505–515.

